CrystEngComm

ROYAL SOCIETY OF CHEMISTRY

PAPER

View Article Online
View Journal | View Issue

Cite this: *CrystEngComm*, 2020, **22**, 7252

Chirality-dependent supramolecular synthons based on the 1,3-oxazolidin-2-one framework: chiral drugs mephenoxalone, metaxalone and 114 other examples†

Alexander A. Bredikhin, * Zemfira A. Bredikhina and Aidar T. Gubaidullin

Received 24th January 2020,
Accepted 19th February 2020

DOI: 10.1039/d0ce00116c

rsc.li/crystengcomm

In four of the five crystalline modifications of the muscle relaxants mephenoxalone **3** and metaxalone **2**, chain supramolecular motifs of three different types are realized. The centrosymmetric cyclic dimer, which is considered typical of amides, was found only once. To clarify the nature of the emerging supramolecular synthons, the set of 119 crystal structures of 1,3-oxazolidin-2-one **1** derivatives, to which drugs **2** and **3** belong, were selected from the Cambridge Structural Database. Analysis of the sample showed that oxazolidinone fragments predominantly form closed ring synthons in racemic crystals, whereas linear chains are typical for enantiopure ones. Thus, in the case of chiral objects, the transition from racemic to enantiopure crystal serves as a powerful tool for designing crystals with a given organization of supramolecular synthon. Two earlier unidentified kryptoracemates (false conglomerates), QEFJAP and QEFJUJ, were found among the analyzed set. Apparently, these are the first representatives of oxazolidinones exhibiting this rare property.

Introduction

The 1,3-oxazolidin-2-one framework (Scheme 1, **1**) is widely used in the development of active pharmacological ingredients (APIs), such as the antibiotics linezolid[1] and tedizolid,[2] fungicide oxadixyl,[3] antimigraine drug zolmitriptan [ref. 3, p 1754], antidepressants befloxatone [ref. 3, p 169] and toloxatone [ref. 3, p 1636] and several others. The popular muscle relaxants metaxalone[4] (Scheme 1, **2**) and mephenoxalone (Scheme 1, **3**) [ref. 3, p 1011] also belong to the chemotype of substituted oxazolidinones.

Most derivatives of oxazolidinone **1** (in particular, all of the above APIs) are chiral. Since the beginning of our century, new chiral APIs have been represented mainly by single enantiomeric compounds,[5] and this trend can be regarded as long-term. Thus, from 45 new drugs approved in the USA in 2015, 12 were complex biological products of the protein or other nature, 33 were individual chiral compounds and, with only one exception, were pure enantiomers.[6] This trend can be seen in subsequent years. Thus, according to a review,[7] in 2018, 30 new chiral APIs of a monomeric nature were registered, of which only two are allowed as racemates.

Recently, spontaneous resolution of enantiomers during crystallization has been increasingly used to obtain enantiopure APIs.[8] To implement this promising approach, it is necessary that either the target product or its key chiral precursor crystallizes as a conglomerate.[9] Earlier, we found that the API guaifenesin (Scheme 1, **4**) is prone to spontaneous resolution and can be obtained in enantiopure forms from the racemate by the entrainment method.[10,11] Recently, this approach has been improved in the work of Lorenz *et al.*, where it was proposed to obtain guaifenesin enantiomers using the effective coupled preferential crystallization-selective dissolution process.[12] Guaifenesin is a synthetic precursor for a whole set of chiral APIs and, in particular, it is possible to obtain pure mephenoxalone **3** enantiomers on its basis.[13]

The tendency to replace racemic APIs with single enantiomeric ones is caused by the fact that the enantiomers of chiral substances, having different spatial organization, interact differently with the chiral receptors of a living organism. Moreover, the crystalline structures of enantiomers and racemates are fundamentally different. Thus, because most of the APIs are used in crystalline forms, their enantiomeric composition affects the bioavailability of the

Arbuzov Institute of Organic and Physical Chemistry, FRC Kazan Scientific Center of RAS, Arbuzov St., 8, Kazan 420088, Russian Federation. E-mail: baa@iopc.ru; Fax: +7 843 273 1872; Tel: +7 843 273 9365

† Electronic supplementary information (ESI) available: CCDC links for compounds *rac*-**3** and (*R*)-**3**, refcodes, chemical names, references to primary literature sources for compounds used in statistical analysis (Table S1). Tables of racemic (Table S2) and enantiomeric crystals (Table S3) for which linear or cyclic supramolecular synthons have been identified. CCDC 1907688 and 1907689. For ESI and crystallographic data in CIF or other electronic format see DOI: 10.1039/d0ce00116c

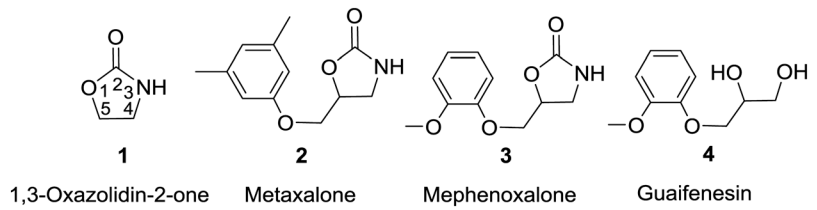

Scheme 1 Molecular structure of muscle relaxants **2** and **3** and related compounds.

final dosage form. This leads to the need for reliable knowledge of the molecular and crystalline structure of enantiopure and racemic substances.

Some time ago we have investigated the thermochemical characteristics of racemic and enantiopure samples of mephenoxalone. It was shown that it crystallizes as a typical racemic compound, and the enantiomeric composition of the eutectic (ee_{eu} = 0.85) prevents the enantiomeric enrichment of mephenoxalone samples with a basic enantiomer content below 92% through recrystallization.[13] The crystal structure of mephenoxalone has not been previously studied by SC XRD, and we considered it necessary to fill this gap for racemic and enantiopure modifications of **3**. Recently, with our participation, the crystal structure and a peculiar phase behavior were investigated for crystalline samples of metaxalone **2** and its enantiopure analogue.[14,15] Comparison of the structural features of compounds **2** and **3** revealed in this way served as a starting point for generalizing some chirality-dependent properties of the supramolecular synthons based on the O=C–N–H fragment of the oxazolidinone **1** and its derivatives.

Experimental

Instrumentation

Optical rotations were measured on a PerkinElmer model 341 polarimeter (concentration *c* is given as g/100 mL). HPLC analyses were performed on a Shimadzu LC-20AD system controller, using a UV detector at 275 nm. The column used, from Daicel, Inc., was Chiralcel OD (0.46 × 25 cm).

Sample preparation

Racemic and (*R*)-5-(2-methoxyphenoxymethyl)-2-oxazolidinones, that is *rac*- and (*R*)-mephenoxalone **3**, were prepared by heating urea with racemic or (*R*)-guaifenesin **4**, (3-(2-methoxyphenoxy)propane-1,2-diol), respectively:[13] *rac*-**3**, mp 141–142 °C (ethanol); (*R*)-**3**, mp 125–127 °C ($CHCl_3$); $[\alpha]_D^{20}$ = −33.5 (*c.* 1.0, EtOH), >99% ee.

Crystals suitable for SC-XRD were grown by slow evaporation of sample solutions from a mixture of $CHCl_3$/CCl_4.

Single crystal X-ray analysis

The single crystal X-ray diffraction data were collected on a Bruker Kappa Apex II CCD diffractometer using monochromated Mo-Kα (0.71073 Å) radiation at 100 K (crystal (*R*)-**3**) and Cu-Kα (1.54178 Å) radiation at 296 K (crystal *rac*-**3**). The crystal data, data collection, and the refinement parameters are given in Table 1.

The structure was solved by direct methods using SHELXS and refined by full-matrix least-squares using SHELXL programs.[16] All nonhydrogen atoms were refined anisotropically. The position of the hydrogen atom of the NH group was determined based on the electron density distribution and was refined isotropically. Other hydrogen atoms were inserted at calculated positions and refined as riding atoms. Data collection: images were indexed and integrated using the APEX2 data reduction package.[17] All calculations were performed on a PC using the WinGX suite of programs.[18] Analysis of the intermolecular interactions was performed using the program PLATON.[19] The Mercury program package[20] was used for figure preparation.

Table 1 Experimental crystallographic data for *rac*-mephenoxalone (*rac*-**3**) and (*R*)-mephenoxalone ((*R*)-**3**)

Compound, sample	*rac*-**3**	(*R*)-**3**
Formula	$C_{11}H_{13}NO_4$	$C_{11}H_{13}NO_4$
M (g mol^{-1})	223.22	223.22
Temperature (K)	296(2)	100(2)
Crystal class	Orthorhombic	Monoclinic
Space group	$Pca2_1$	$P2_1$
Crystal size (mm^3)	0.14 × 0.23 × 0.31	0.11 × 0.18 × 0.76
Z, Z'	4, 1	2, 1
Cell parameters	a = 19.5781(11) b = 9.8640(6) c = 5.5937(3)	a = 9.7048(7) Å b = 5.5085(4) Å c = 10.4326(7) Å β = 108.560(4)°
V (Å^3)	1080.25(11)	528.71(7)
Radiation, wavelength λ (Å)	CuK$_\alpha$, λ = 1.54178	MoK$_\alpha$, λ = 0.71073
F(000)	472	236
ρ_{calc} (g cm^{-3})	1.373	1.402
μ (mm^{-1})	0.884	0.108
θ range (deg)	4.482–70.027	3.472–30.608
Reflections measured	18 683	9737
Independent reflections/R(int)	1513/0.0302	2692/0.0460
Number of parameters/restraints	182/1	150/1
Reflections [$I > 2\sigma(I)$]	1482	2181
R_1/wR_2 [$I > 2\sigma(I)$]	0.0238/0.0643	0.0410/0.0756
R_1/wR_2 (all reflections)	0.0243/0.0648	0.0650/0.0811
Goodness of fit on F^2	1.043	1.018
ρ_{max}/ρ_{min} (e Å^{-3})	0.117/−0.092	0.217/−0.233

Crystallographic data for *rac*-**3** and (*R*)-**3** have been deposited with the Cambridge Crystallographic Data Centre as supplementary publication numbers CCDC 1907688 and 1907689, respectively.

Results and discussion

The structure of mephenoxalone crystalline modifications

Racemic mephenoxalone **3** crystallizes in the orthorhombic system in the space group $Pca2_1$ (no. 29). Enantiopure (*R*)-**3** crystallizes in the monoclinic system in the group $P2_1$ (4). In both cases, a single symmetrically independent molecule is present in the asymmetric unit ($Z' = 1$). Other details of the X-ray experiment are shown in Table 1.

As shown in Fig. 1, the conformation of molecule **3** is the same for both crystals.

When analyzing the internal organization of crystalline modifications of muscle relaxants **2** and **3**, we will rely on the concept of supramolecular synthon (SS) proposed by Gautam Desiraju a quarter of a century ago.[21] As follows from this, as well as from the later reviews,[22–25] the fragment A═X–D–H (A═X is a HB acceptor, D–H is a HB donor) is among the most popular "synthon-forming" molecular fragments, typical examples of which are carboxyl and amide groups, O═C–O–H and O═C–N–H. The latter presents in molecules **2** and **3**. Both amide and carboxylic fragments are capable of forming zero-dimensional cyclic and one-dimensional chain-like synthons (Scheme 2). It was repeatedly noted that cyclic supramolecular structures **I** and **III** substantially dominate. In those rare cases when, in a family of structurally related carboxylic acids, a predominance of chain motifs was detected, this fact was explained by the presence in the structure of the studied molecules of substituents capable of stabilizing a "non-standard" linear synthon due to specific interactions.[26]

For designating patterns of hydrogen bonds that are realized in crystals of organic compounds, in continuation of the work of Margaret Etter,[27] Joel Bernstein *et al.* developed a system of descriptors based on the concept of a multilevel graph.[28] Such a representation of the supramolecular synthon, being a significant step towards systematization of a large amount of dissimilar information, has a too general nature and masks the differences in the hydrogen bonding system, which are important in analyzing narrower molecular sets. For example, the single descriptor $\mathbf{C}_1^1(4)$ (or simply **C(4)**) designates chain-forming H-bonded dimers for SS **II** and **IV** (Scheme 2) that differ significantly in terms of their "chemical composition". In the present paper we will deal with the only synthon-forming element, namely, the O═C–N–H fragment included in the 1,3-oxazolidin-2-one cycle. In such a well-defined situation, there is no need to specify an element in the synthon descriptor. However, some extensions will be required to reflect the stereochemical and crystallographic features of the crystal packing. The point is that planar graphs (graphs that can be drawn in the plan without edges crossing), describing the allocation of bonds in the majority of three-dimensional chemical compounds (for example, Schlegel diagrams for fullerenes), are achiral. Since chirality plays a fundamental role in crystallography, then in the framework of further discussion, we will supply the standard descriptors with the prefixes *hm-* and *ht-* specifying the homochiral and heterochiral supramolecular constructs, respectively. In the first ones, all the elements forming them have a common configuration; the element configurations alternate in the second ones.

After these introductory remarks, let us return to our crystals. In both cases studied in this work, hydrogen bonds in crystals generate one-dimensional (1D) infinite zigzag chains, shown in Fig. 2 and 3. However, it is obvious that these motifs are not identical.

As can be seen from Fig. 2, in *rac*-**3** crystals, infinite 1D chains are formed along the glide plane **c** with opposite enantiomers alternating in a chain; it can be said that in this case a *ht*-**C(4)** synthon is formed. On the contrary, in the case of (*R*)-**3** crystals (Fig. 3), one-dimensional chains, formed along the 2_1 screw axes, consist of identical enantiomers, so SS should be called *hm*-**C(4)**.

Different ways of forming the supramolecular motif cause different properties of the final crystal structure. For example, the racemic crystal packing density (Kitaigorodsky packing index) is 69.1%, whereas the enantiopure crystal KPI = 71.2%. Despite its greater density, enantiopure mephenoxalone packing, as such, is inferior to the racemic one in energy, ΔG^0 = 3.8 kJ mol^{-1}.[13] However, it should be noted that the X-ray experiment for the two structures was carried out at significantly different temperatures (Table 1), so a direct comparison of the KPI in this case must be treated with caution.

Previously, homochiral chain synthons were detected in enantiopure metaxalone (*S*)-**2** crystals (group $P2_12_12_1$ (19); CSD refcode WISNEU) and polymorph A of racemic metaxalone A-*rac*-**2** ($P\bar{1}$ (2); AXOGAW).[14,15] In the first case, the motif *hm*-**C(4)** (the same in nature with that in Fig. 3) is formed around the screw axis 2_1.

In the second case, the only existing symmetry element, the inversion center, is not able to form any homochiral constructs. However, two independent molecules A and B, each of which has the same configuration, present in the A-*rac*-**2** asymmetric unit. They alternate along the homochiral

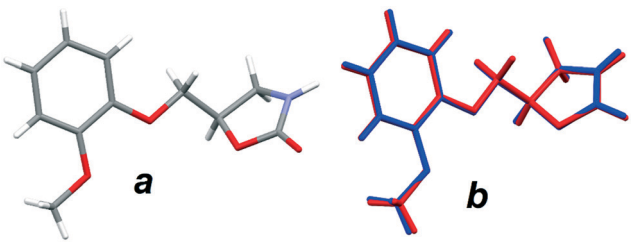

Fig. 1 Mephenoxalone **3** molecule in the different crystalline modifications. (a) (*R*)-Enantiomer in *rac*-**3** crystals. (b) Overlay of (*R*)-enantiomers presenting in *rac*-**3** crystals (red) and in (*R*)-**3** crystals (blue).

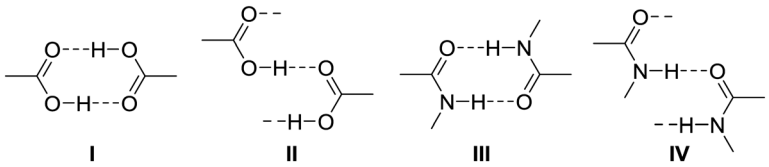

Scheme 2 Ring- and chain-like synthons for carboxylic and amide functions.

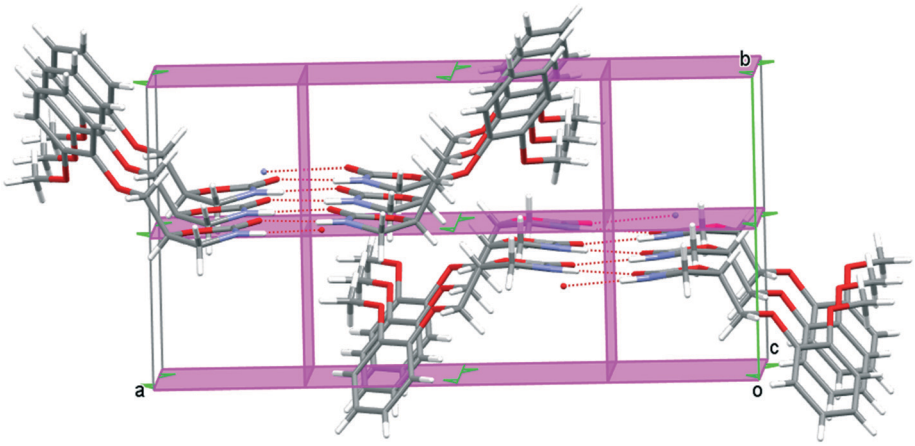

Fig. 2 Two one-dimensional chains of H-bonded molecules in the crystals of racemic mephenoxalone *rac*-**3**.

chains parallel to the shortest axis *a*. The resulting SS (Fig. 4) is similar to the one shown in Fig. 3, but the subunits A and B of this construct are not connected by any symmetry element. Strictly speaking, a kind of heterosynthon[23,24] arises when several independent molecules (A, B, *etc.*) alternate within a single synthon, and the common chain is a sequence of intermolecular H-bonds {···O2A═C2A–N3A–H3A···O2B═C2B–N3B–H3B···}. This feature can be reflected using additional indices, and the SS realized in A-*rac*-**2** crystals could be designated as *hm*-$\mathbf{C}_2^2(\mathbf{8})$:A/B. In the crystals of the most stable[15] metaxalone polymorph B-*rac*-**2** ($P2_1/c$ (14); AXOGAW01), the supramolecular synthon is a heterochiral centrosymmetric ring (Fig. 5) denoted as *ht*-$\mathbf{R}_2^2(\mathbf{8})$.

Thus, in the five cases analyzed above, the most expected for amide ring synthon **III** (Scheme 2) was realized once only, while one-dimensional chains were realized in four cases and were represented by three different variants. Whether such a distribution is a random feature of a small data set, or whether we are dealing with the essential properties of the

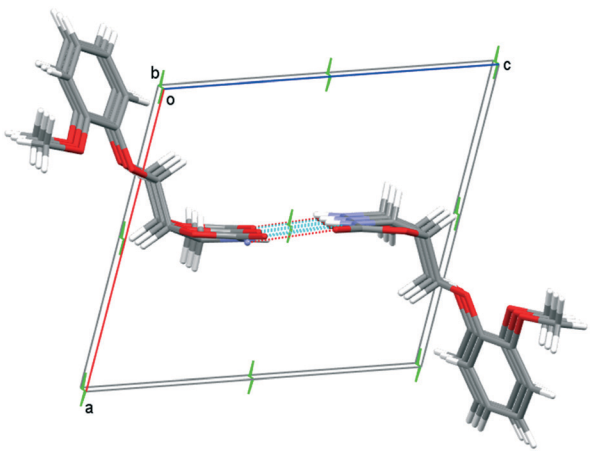

Fig. 3 Oriented along the 0*b* axis, a one-dimensional chain of H-bonded molecules in crystals of enantiopure mephenoxalone (*R*)-**3**.

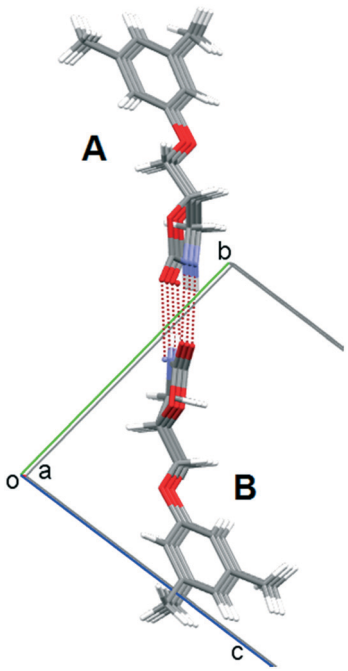

Fig. 4 One-dimensional homochiral supramolecular synthon in A-*rac*-**2** crystals.

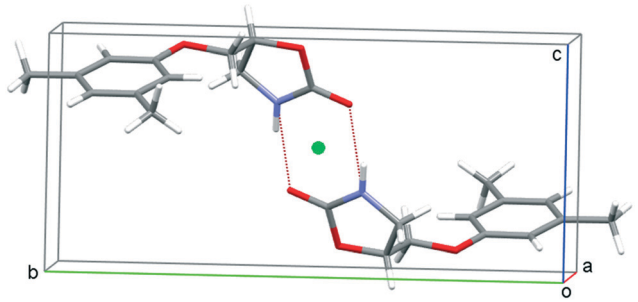

Fig. 5 Zero-dimensional heterochiral supramolecular motif in B-*rac*-**2** crystals.

oxazolidinone cycle, we will try to find out below, on the example of a more representative sample of related structures.

Rings *vs.* chains. First approximation

To analyze the primary supramolecular assemblies in 1,3-oxazolidin-2-one crystals, we sampled compounds with this skeleton from the Cambridge Structural Database (CSD version 5.40 updates Feb 2019). From the data set, 3-substituted derivatives were filtered out because they contain no N–H key fragment. Polymeric, organometallic and ionic derivatives as well as structures for which there was no information about 3D coordinates were filtered out too. From the resulting array (248 hits), structures that contained other donor (NH, OH, SH, *etc.*) and acceptor (C═O, N═O, S═O, *etc.*) fragments, actively forming their own supramolecular motifs, were removed manually. To the remaining set, our data on compounds *rac*-**3** and *R*-**3** were added. The selected 119 hits, their refcodes, chemical names and references to primary sources are given in Table S1.†

As mentioned in the Desiraju review,[24] "a synthon is a probabilistic event. The more often it is seen, the more likely it will be seen in the crystal structure of new molecules that contain the requisite functional groups". Further, we will analyze the frequency (read – the probability) of the realization of one or another type of SS among the crystals of oxazolidinone derivatives. In a total array of 119 oxazolidinones, 0D dimer ring synthons occur 45 times, and 1D linear chain synthons 74 times.

At first glance, against expectations, statistics indicate the predominance of type **IV** catemers over type **III** rings. And in this sense, the result obtained for a small sample of crystalline modifications of oxazolidinones **2** and **3** corresponds to the results obtained in the analysis of the general array. However, the apparent contradiction with the generally accepted opinion makes us think about the methodology of direct statistical analysis itself, which apparently does not take into account some significant factors. We believe that since all oxazolidinones are chiral in crystals, this factor is the enantiomeric composition of the analyzed sample.

Both the cyclic and the linear synthons can be formed in various ways. Their organization seems most natural around the symmetry elements (closed in the case of rings and open in the case of chains) present in the crystal.

Generally speaking, the dimer **III** can form a symmetrical ring around the rotational axis of the second order or around the center of inversion. In the first case, the homochiral synthon *hm*-$\mathbf{R_2^2(8)}$ arises, and in the second, the heterochiral synthon *ht*-$\mathbf{R_2^2(8)}$. The presence of several molecules in the asymmetric unit of the cell ($Z' > 1$), preserving all the ways just listed, creates additional possibilities for the formation of rings from symmetrically independent molecules, both in the homo- and in the heterochiral variants. However, with all the variety of choices, the majority (32 out of 45) of ring synthons **III** identified in the general set belong to the type *ht*-$\mathbf{R_2^2(8)}$ and are formed around the inversion center. Chain motifs can mainly be formed around the screw axes of any order and along the glide planes. In the first case, a homochiral synthon *hm*-**C(4)** is obtained, in the second case, heterochiral synthon *ht*-**C(4)**. As in the case of cyclic synthons, an increase in the number of symmetrically independent molecules ($Z' > 1$) expands the possibilities of forming chains due to the association of symmetrically independent molecules in various combinations. Herewith, out of 75 identified 1D catemers, 64 (>85%) belong to the first type.

In crystals of achiral substances, any elements of symmetry can be realized. Rotational and screw axes can be realized in crystals of chiral substances regardless of their enantiomeric composition. In contrast, centers of inversion and glide planes can only be present in racemic crystals. Obviously, "inequality" of symmetry elements, the ban on the important ones in enantiopure crystals, makes it mandatory to analyze the frequency of linear and cyclic synthons in arrays of racemic and enantiopure crystals separately.

It was stated that oxazolidinones are chiral in crystals, but it is not always clear from the information presented in the CSD whether the original polycrystalline specimen was racemic or enantiopure. However, it is quite possible to estimate the "enantiomeric composition" of the set. Of the 119 structures represented in the sample, 68 crystallize in Sohncke space groups and 51 in the "non-Sohncke" ones. Single-enantiomeric samples can crystallize only in Sohncke space groups. A racemic substrate can crystallize in a Sohncke group only in two fairly rare cases: first, when a substance prone to spontaneous resolution crystallizes as a conglomerate of pure enantiomers.[29,30] In this case, for a researcher who deals only with the final crystal structure, information about the enantiomeric composition of the initial sample is lost, but the single-enantiomeric nature of the crystal which was analyzed is quite reliable.

The second possibility is associated with the formation by a racemate of the crystalline form of a kryptoracemate[31] (another name for a false conglomerate[30,32]) when there are 2N independent molecules in the asymmetric unit of the crystal, of which N is represented by one enantiomer and the same number by the opposite. In our set, we found two such compounds, QEFJAP and QEFJUJ (Scheme 3). This fact was not noted in the original publication.[33]

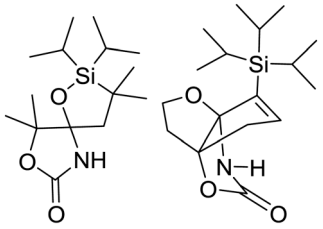

QEFJAP QEFJUJ

Scheme 3 Molecular structure of two previously unidentified kryptoracemates.

Taking this into account, it can be assumed that the sample includes 53 (45%) racemic and 66 (55%) enantiopure crystalline samples. In a manner, the sample is slightly biased, but this deviation is unlikely to affect the final conclusions.

Supramolecular synthons in a subsample of racemic crystals

The list of refcodes of 53 compounds in this secondary set, information about the space group, the number of independent molecules (Z'), and the identified type of PSM are given in Table S2.† The chemical structures of the compounds, refcodes of which are mentioned in the text, are shown in Scheme 4.

In 38 out of 53 subset compounds, SS are closed 0-dimensional cyclic structures. It can be argued that in the crystals of racemic 1,3-oxazolidin-2-ones, 0D cyclic synthons noticeably, about three times, prevail over 1D catemers. In the simplest case, when $Z' = 1$ (29 examples), rings are described by the graph *ht*-$\mathbf{R_2^2(8)}$. If two independent molecules are present in the asymmetric unit ($Z' = 2$), the motif can just double, and each independent molecule forms its own zero-dimensional SM of type *ht*-$\mathbf{R_2^2(8)}$:A and *ht*-$\mathbf{R_2^2(8)}$:B (KULHAC and TEWHIM, $P\bar{1}$ (2); WOYTAF, $P2_1/c$ (14), Scheme 4).

In four cases, including kryptoracemates QEFJAP and QEFJUJ (Scheme 3), a *ht*-$\mathbf{R_2^2(8)}$:A/B synthon is formed by different symmetry-independent molecules having opposite configurations (Fig. 6). Naturally, in such cases, the cyclic dimer does not have its own symmetry. The formation of the homochiral ring *hm*-$\mathbf{R_2^2(8)}$ around the symmetry axis 2 is even more exotic and is realized only in two structures, PENWEL and QUFHII (Scheme 4), which crystallize in centrosymmetric $C2/c$ (15) and non-centrosymmetric $Iba2$ (45) groups, respectively.

Catemers in crystals of racemic oxazolidinones are represented by 15 examples. Most often (9 times), *hm*-**C(4)** catemers of homogeneous elements are formed around the screw axes 2_1. Note that this motif is realized in crystals of the first term of this chemotype, *i.e.* the unsubstituted heterocycle **1** (OXAZIL11, Scheme 1). Another possibility of the formation of a homochiral chain in a racemic crystal appears in the case of an increase in the number of symmetrically independent molecules in an asymmetric unit. Above, using the example of A-*rac*-**2** (Fig. 4), we have analyzed in detail the motif *hm*-$\mathbf{C_2^2(8)}$:A/B formed in this way.

In the studied array examples of heterochiral chains, *ht*-**C(4)** are found only five times. Heterochiral catemers are formed along glide planes in all the detected cases. In addition to the above presented racemic mephenoxalone *rac*-**3** (Fig. 2), these are (see Scheme 4) EFEJIJ ($P2_1/c$ (14)), MUXLUN ($P2_1/a$ (14)), WIKCUO ($Pca2_1$ (29)) and RESSUD ($Pna2_1$ (33)). In the case of RESSUD crystals, there are two independent molecules in the asymmetric unit, and one should speak of two independent motifs *ht*-**C(4)**:A and *ht*-**C(4)**:B.

Supramolecular synthons in a subsample of enantiomeric (enantiopure) crystals

The list of refcodes of 66 compounds of this subset, their space groups, the number of independent molecules (Z'), and the identified type of SS are listed in Table S3.† According to the selection conditions, in all crystals listed in this table the molecules with a common configuration are present, and, therefore, any supramolecular motifs formed in the crystal can only be homochiral.

In the total array of analyzed structures, in 59 cases (89%) chain-like *hm*-**C** primary supramolecular motifs were identified, *i.e.*, such motifs turn out to be predominant. As expected, most often such a motif is built around a second-order screw axis 2_1, mostly in the groups $P2_1$ (4) (21 times) and $P2_12_12_1$ (19) (31 times). A rare case of the *hm*-**C(4)** motif organized around a higher-order screw axis is found in VIPJOV crystals (Scheme 4 and Fig. 7a). In this case, the conventionally one-dimensional *hm*-**C(4)** motif is organized around the chiral screw axis 4_3 (group $P4_3$ (78); Fig. 7b) and acquires a kind of tertiary structure, namely the left *M*-helix (Fig. 7c). Let us draw the reader's attention to the fact that a spatial organization of a chain-like supramolecular ensemble formed around a second-order screw axis can also vary from a flat zigzag to a well-developed three-dimensional helix.

As analysis shows, the simplest version of the *hm*-$\mathbf{C_2^2(8)}$ motif is realized in enantiopure crystals in the case of $Z' = 1$. An increase in the number of symmetrically independent molecules in the asymmetric unit of the crystal cell can lead to a simple doubling of the motif, as is the case for AKUXOT and CUPJIG01 (Scheme 4, $P2_1$ (4), $Z' = 2$ for both), wherein each independent molecule forms a catemer, consisting only of its own kind. A variant of alternating independent molecules in a common chain motif is also possible. Thus, SS *hm*-$\mathbf{C_2^2(8)}$:A/B are realized in RADCUX ($P2_1$ (4)), LIRMIJ and MEYWEU (Scheme 4, both $P2_12_12_1$ (19)) crystals. In the asymmetric unit of CEMDAB crystals ($P1$ (1), Scheme 4) there are four independent molecules with a common configuration. The molecules are combined in one-dimensional associates in pairs, generating symmetrically unrelated motifs *hm*-$\mathbf{C_2^2(8)}$:A/B and *hm*-$\mathbf{C_2^2(8)}$:C/D.

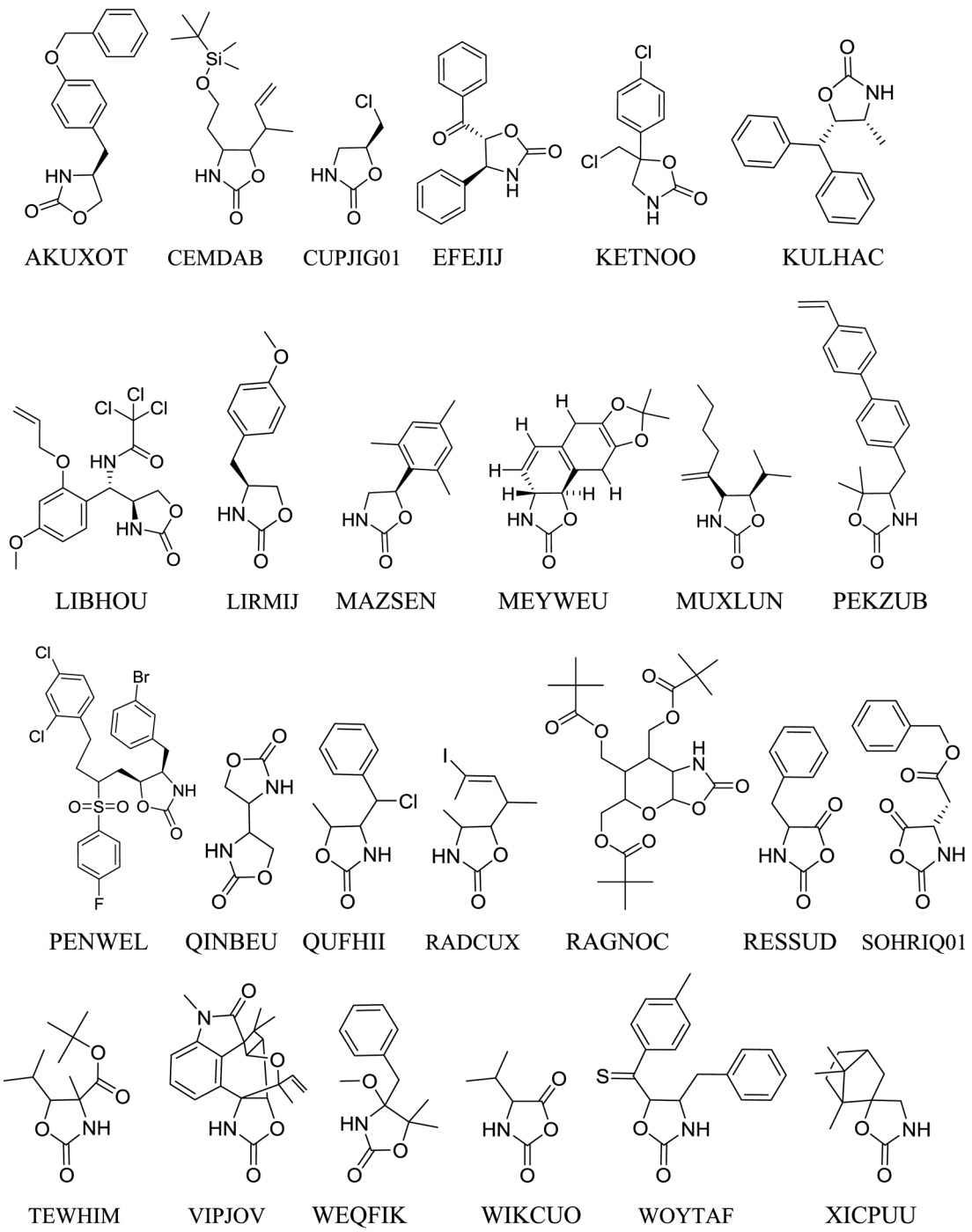

Scheme 4 Chemical structure of the compounds, refcodes of which are discussed in the text. Refcodes are listed in alphabetical order.

In six of the seven remaining cases, MAZSEN, PEKZUB, LIBHOU, XICPUU, KETNOO, and RAGNOC ($P2_1$ (4), $P2_1$ (4), $C2$ (5), $P2_12_12$ (18), $P2_12_12_1$ (19), and $P2_12_12_1$ (19) in the order listed; Scheme 4), there are two symmetry-independent molecules in the crystals. In all these cases, independent A and B molecules are combined in the *hm*-$\mathbf{R}_2^2(\mathbf{8})$:A/B rings. In the WEQFIK crystals ($P1$ (1), Scheme 4) there are 4 independent A, B, C and D molecules, so two independent 0-dimentional motifs, *hm*-$\mathbf{R}_2^2(\mathbf{8})$:A/B and *hm*-$\mathbf{R}_2^2(\mathbf{8})$:C/D, are implemented.

Conclusions

It is generally accepted that in the crystals of carboxylic acids and amides 0D cyclic dimers are preferred over 1D catemers. The chiral muscle relaxant mephenoxalone **3** belongs to the class of substituted 1,3-oxazolidin-2-ones **1** (Scheme 1) and has an amide fragment O═C–N–H in its structure. During SC XRD analysis of racemic and enantiomeric mephenoxalone it was shown that the directed intermolecular hydrogen bonds

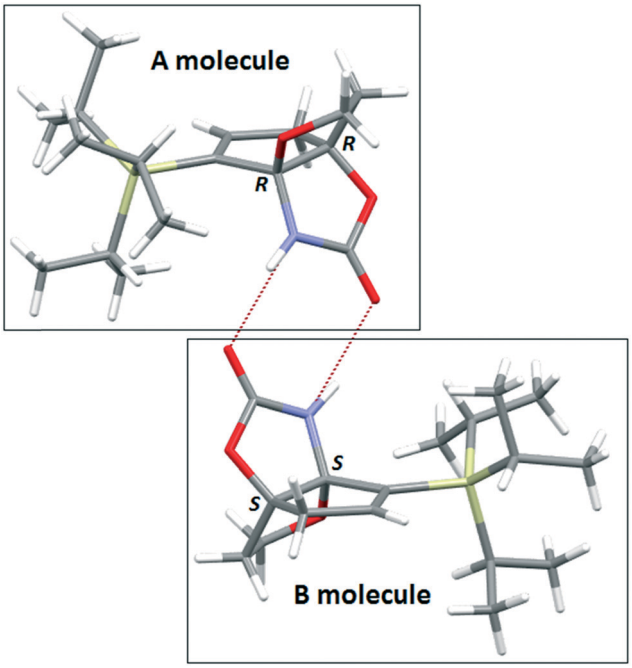

Fig. 6 Zero-dimensional supramolecular motif *ht*-$\mathbf{R}_2^2(8)$:A/B in the crystals of the kryptoracemate QEFJUJ belonging to the Sohncke space group $P2_12_12_1$.

{···O2═C2–N3–H3···O2′═C2′–N3′–H3′···} play a decisive role in the formation of crystal packing, but in both crystals only **C(4)** chains, differing in the way of their organization, were registered. The third variant of the chain construction was earlier found for the A-*rac*-**2** crystalline form of the muscle relaxant metaxalone **2** belonging to the same chemotype. In total, out of five identified crystalline modifications of **2** and **3**, in only one case, namely in B-*rac*-**2** crystals, a cyclic synthon $\mathbf{R}_2^2(8)$ was detected.

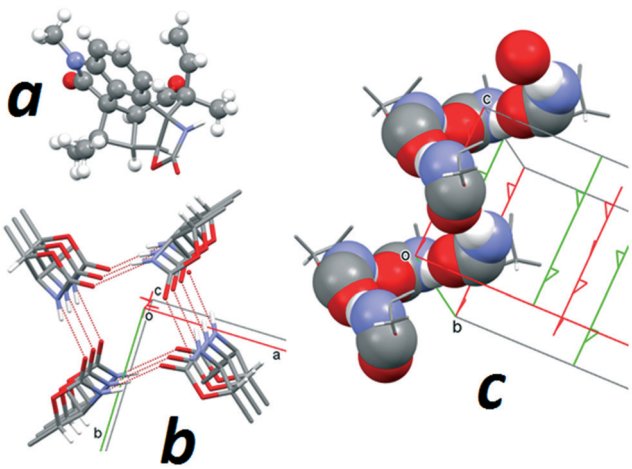

Fig. 7 Supramolecular motif in VIPJOV crystals. (a) Independent molecule; the "caped sticks" style is used to highlight a fragment, further depicted in (b) and (c). (b) One-dimensional supramolecular synthon *hm*-**C(4)**, organized around a screw axis 4_3. (c) The same motif; the O═C–N–H fragment is marked by the "space fill" style.

To identify the circumstances that control the formation of chain or ring supramolecular motifs within the oxazolidinone **1** chemotype, an array of 119 structures was selected from the Cambridge Structural Database, where the supramolecular motifs in the crystals were formed by the interaction of the amide O═C–N–H fragments. In this set, as well as in a small sample of crystals **2** and **3**, chain-like synthons also prevail over ring-like ones in the ratio 74 : 45. Since the synthon-forming symmetry elements are unevenly distributed in the arrays of racemic and enantiopure samples, we investigated the distribution of chains and rings separately in samples of racemic and enantiomeric crystals. As one might expect, in a subset of 53 racemic crystals, ring synthons prevail over catemers in a ratio of ~4 : 1. At the same time, in a subset of 66 enantiopure crystals, preferences change diametrically, and already the catemers prevail over the rings in a ratio of ~8 : 1. Based on these data, it can be argued that in the case of chiral objects, not only and not so much the nature of substitution, but first of all the change in chirality characteristics, namely the transition from racemic to enantiopure crystal, serves as a powerful tool for designing crystals with a given organization of supramolecular synthon.

Returning to the muscle relaxants **2** and **3**, with which this work began, it can be noted that the dominance of linear motifs in their crystals, firstly, is normal for a small set, and, secondly, reflects the trend noted by us for a larger sample. In light of the above, another feature seems remarkable: in the tiny array of 5 crystalline modifications of mephenoxalone and metaxalone, all possible variants of catemers (*hm*-**C(4)** in (*R*)-**3** and (*S*)-**2** crystals, *ht*-**C(4)** in *rac*-**3** crystals, and heterosynthon $\mathbf{C}_2^2(8)$:A/B in crystals of A-*rac*-**2**), found for the entire sample studied in this work, were realized.

To conclude this section, recall that as a "by-product" of analyzing a representative set of substituted oxazolidinones, we have found two earlier unreported kryptoracemates (false conglomerates), compounds QEFJAP and QEFJUJ (Table S1† and Scheme 3). Apparently, these are the first representatives of this chemotype exhibiting this rare property.

Conflicts of interest

There are no conflicts to declare.

Acknowledgements

The authors are grateful to the Assigned Spectral-Analytical Center of FRC Kazan Scientific Center of RAS for technical assistance in research.

References

1 S. M. Hashemian, T. Farhadi and M. Ganjparvar, Linezolid: a review of its properties, function, and use in critical care, *Drug Des., Dev. Ther.*, 2018, **12**, 1759–1767, DOI: 10.2147/DDDT.S164515.

2 O. Ferrandez, O. Urbina and S. Grau, Critical role of tedizolid in the treatment of acute bacterial skin and skin structure infections, *Drug Des., Dev. Ther.*, 2017, **11**, 65–82, DOI: 10.2147/DDDT.S84667.
3 *The Merck Index*, ed. M. J. O'Neil, Merck and Co., Whitehouse Station, NJ, USA, 14th edn, 2006, p. 1191.
4 S. See and R. Ginzburg, Skeletal muscle relaxants, *Pharmacotherapy*, 2008, **28**, 207–213, DOI: 10.1592/phco.28.2.207.
5 H. Murakami, From racemates to single enantiomers - Chiral synthetic drugs over the last 20 years, *Top. Curr. Chem.*, 2007, **269**, 273–299, DOI: 10.1007/128_2006_072.
6 A. Calcaterra and I. D'Acquarica, The market of chiral drugs: Chiral switches versus de novo enantiomerically pure compounds, *J. Pharm. Biomed. Anal.*, 2018, **147**, 323–340, DOI: 10.1016/j.jpba.2017.07.008.
7 B. G. de la Torre and F. Albericio, The pharmaceutical industry in 2018. An analysis of FDA drug approvals from the perspective of molecules, *Molecules*, 2019, **24**, 809, DOI: 10.3390/molecules24040809.
8 A. A. Bredikhin and Z. A. Bredikhina, Stereoselective crystallization as a basis for single-enantiomer drug production, *Chem. Eng. Technol.*, 2017, **40**, 1211–1220, DOI: 10.1002/ceat.201600649.
9 G. Coquerel, Chiral discrimination in the solid state: Applications to resolution and deracemization, in *Advances in Organic Crystal Chemistry*, ed. R. Tamura and M. Miyata, Springer Japan, 2015, pp. 393–420, DOI: 10.1007/978-4-431-55555-1_20.
10 Z. A. Bredikhina, V. G. Novikova, D. V. Zakharychev and A. A. Bredikhin, Solid state properties and effective resolution procedure for guaifenesin, 3-(2-metoxyphenoxy)- 1,2-propanediol, *Tetrahedron: Asymmetry*, 2006, **17**, 3015–3020, DOI: 10.1016/j.tetasy.2006.10.027.
11 A. A. Bredikhin, A. T. Gubaidullin, Z. A. Bredikhina, D. B. Krivolapov, A. V. Pashagin and I. A. Litvinov, Absolute configuration and crystal packing for three chiral drugs prone to spontaneous resolution: Guaifenesin, methocarbamol and mephenesin, *J. Mol. Struct.*, 2009, **920**, 377–382, DOI: 10.1016/j.molstruc.2008.11.037.
12 E. Temmel, M. J. Eicke, F. Cascella, A. Seidel-Morgenstern and H. Lorenz, Resolution of racemic guaifenesin applying a coupled preferential crystallization-selective dissolution process: rational process development, *Cryst. Growth Des.*, 2019, **19**, 3148–3157, DOI: 10.1021/acs.cgd.8b01660.
13 A. A. Bredikhin, Z. A. Bredikhina, D. V. Zakharychev and A. V. Pashagin, Chiral drugs related to guaifenesin: synthesis and phase properties of methocarbamol and mephenoxalone, *Tetrahedron: Asymmetry*, 2007, **18**, 1239–1244, DOI: 10.1016/j.tetasy.2007.05.019.
14 S. Aitipamula, P. S. Chow and R. B. H. Tan, Conformational polymorphs of a muscle relaxant, metaxalone, *Cryst. Growth Des.*, 2011, **11**, 4101–4109, DOI: 10.1021/cg200678e.
15 A. A. Bredikhin, D. V. Zakharychev, A. T. Gubaidullin and Z. A. Bredikhina, Solid phase behavior, polymorphism, and crystal structure features of chiral drug metaxalone, *Cryst. Growth Des.*, 2018, **18**, 6627–6639, DOI: 10.1021/acs.cgd.8b00874.
16 G. M. Sheldrick, Crystal structure refinement with SHELXL, *Acta Crystallogr., Sect. C: Struct. Chem.*, 2015, **71**, 3–8, DOI: 10.1107/S2053229614024218.
17 *APEX2 (Version 2.1)*, SAINTPlus. Data Reduction and Correction Program (Version 7.31A), Bruker Advanced X-ray Solutions, BrukerAXS, Madison, WI, 2006.
18 L. J. Farrugia, WinGX suite for small-molecule single-crystal crystallography, *J. Appl. Crystallogr.*, 1999, **32**, 837–838, DOI: 10.1107/S0021889899006020.
19 A. L. Spek, Single-crystal structure validation with the program PLATON, *J. Appl. Crystallogr.*, 2003, **36**, 7–13, DOI: 10.1107/S0021889802022112.
20 C. F. Macrae, P. R. Edgington, P. McCabe, E. Pidcock, G. P. Shields, R. Taylor, M. Towler and J. van de Streek, Mercury: visualization and analysis of crystal structures, *J. Appl. Crystallogr.*, 2006, **39**, 453–459, DOI: 10.1107/S002188980600731X.
21 G. R. Desiraju, Supramolecular synthons in crystal engineering – a new organic synthesis, *Angew. Chem., Int. Ed. Engl.*, 1995, **34**, 2311–2327, DOI: 10.1002/anie.199523111.
22 G. R. Desiraju, Designer crystals: intermolecular interactions, network structures and supramolecular synthons, *Chem. Commun.*, 1997, 1475–1482, DOI: 10.1039/A607149J.
23 O. Almarsson and M. J. Zaworotko, Crystal engineering of the composition of pharmaceutical phases. Do pharmaceutical co-crystals represent a new path to improved medicines?, *Chem. Commun.*, 2004, 1889–1896, DOI: 10.1039/B402150A.
24 G. Desiraju, Crystal Engineering: From Molecule to Crystal, *J. Am. Chem. Soc.*, 2013, **135**, 9952–9967, DOI: 10.1021/ja403264c.
25 A. Mukherjee, Building upon supramolecular synthons: some aspects of crystal engineering, *Cryst. Growth Des.*, 2015, **15**, 3076–3085, DOI: 10.1021/acs.cgd.5b00242.
26 D. Das and G. R. Desiraju, Effects of the substituent on the formation of dimers and catemers in phenylpyruvic acids, *CrystEngComm*, 2006, **8**, 674–679, DOI: 10.1039/B606054D.
27 M. C. Etter, Encoding and decoding hydrogen-bond patterns of organic-compounds, *Acc. Chem. Res.*, 1990, **23**, 120–126, DOI: 10.1021/ar00172a005.
28 J. Bernstein, R. E. Davis, L. Shimoni and N. L. Chang, Patterns in hydrogen bonding - functionality and graph set analysis in crystals, *Angew. Chem., Int. Ed. Engl.*, 1995, **34**, 1555–1573, DOI: 10.1002/anie.199515551.
29 L. Perez-Garcia and D. B. Amabilino, Spontaneous resolution, whence and whither: from enantiomorphic solids to chiral liquid crystals, monolayers and macro- and supramolecular polymers and assemblies, *Chem. Soc. Rev.*, 2007, **36**, 941–967, DOI: 10.1039/B610714A.
30 A. T. Gubaidullin, A. I. Samigullina, Z. A. Bredikhina and A. A. Bredikhin, Crystal structure of chiral *ortho*-alkyl phenyl ethers of glycerol: true racemic compound, normal, false and anomalous conglomerates within the single five-

membered family, *CrystEngComm*, 2014, **16**, 6716–6729, DOI: 10.1039/C4CE00519H.

31 L. Fabian and C. P. Brock, A list of organic kryptoracemates, *Acta Crystallogr., Sect. B: Struct. Sci.*, 2010, **66**, 94–103, DOI: 10.1107/S0108768109053610.

32 R. Bishop and M. L. Scudder, Multiple molecules in the asymmetric unit (Z ' > 1) and the formation of false conglomerate crystal structures, *Cryst. Growth Des.*, 2009, **9**, 2890–2894, DOI: 10.1021/cg9002143.

33 J. L. Shih, S. Jansone-Popova, C. Huynh and J. A. May, Synthesis of azasilacyclopentenes and silanols via Huisgen cycloaddition-initiated C-H bond insertion cascades, *Chem. Sci.*, 2017, **8**, 7132–7137, DOI: 10.1021/cg9002143.